Coatings **2011**, *1*, 3-16; doi:10.3390/coatings1010003

OPEN ACCESS

coatings

ISSN 2079-6412

www.mdpi.com/journal/coatings/

Article

Improvement of the Oxidation Resistance of CoNiCrAlY Bond Coats Sprayed by High Velocity Oxygen-Fuel onto Nickel Superalloy Substrate

Alessio Fossati [1,*], Martina Di Ferdinando [1], Alessandro Lavacchi [2], Andrea Scrivani [3], Carlo Giolli [3] and Ugo Bardi [1]

[1] Consorzio Interuniversitario Nazionale per la Scienza e Tecnologia dei Materiali (INSTM), Via G. Giusti 9, 50121 Firenze, Italy

[2] Istituto di Chimica dei Composti Organometallici (ICCOM-CNR), Via Madonna del Piano 10, 50019 Sesto Fiorentino, Italy

[3] Turbocoating SpA, Via Mistrali 7, 43040 Rubbiano di Solignano, Parma, Italy

* Author to whom correspondence should be addressed; E-Mail: alessio.fossati@gmail.com; Tel.: +39-055-457-311-9; Fax: +39-055-457-312-0.

Received: 1 October 2010; in revised form: 28 October 2010 / Accepted: 23 November 2010 / Published: 26 November 2010

Abstract: CoNiCrAlY powders with similar granulometry and chemical composition, but different starting reactivity toward oxygen, were sprayed onto superalloy substrates by High Velocity Oxygen-Fuel producing coatings of similar thicknesses. After spraying, samples were maintained at 1,273 K in air for different test periods of up to 5,000 hours. Morphological, microstructural, compositional and electrochemical analyses were performed on the coated samples in order to assess the high temperature oxidation resistance provided by the two different powders. The powder with higher starting reactivity towards oxygen improves the oxidation resistance of the coated samples by producing thinner and more adherent thermally grown oxide layers.

Keywords: high velocity oxyfuel (HVOF); oxidation; superalloy; bond coat; protective coating

---

1. Introduction

Thermal barrier coating (TBC) systems are employed in gas turbines in order to reduce thermal exposure of structural components. TBCs are usually composed of a MCrAlY bond coat (with M=Co, Ni or their combination) which provides oxidation resistance and an yttria partially stabilized zirconia (YPSZ) top coat that provides thermal insulation to the metallic substrate; moreover, the bond coat enhances the adhesion of the ceramic top coat.Working conditions lead to the oxidation of the bond coat which causes the development of a Thermally Grown Oxide (TGO) layer at the ceramic/bond coat interface and consume the oxidation resistant element reservoir. TGO formation has been recognized to be one of the main causes for the TBC failure [1-3]. The failure of the TBC systems critically depends on the characteristics of the TGO layer. If this layer is composed of a compact, continuous and adhesive alumina (Al_2O_3) scale, it acts as a diffusion barrier thus reducing the extent of further oxidation of the bond coat; more over, the alumina scale can suppress or reduce the growth of other detrimental oxides improving the system service life [4-7]. Many researches showed that TBC failures can be correlated to the reaching of a TGO critical thickness [1,8]. Thus, the reduction of TGO growth can have a significant impact on the durability of a TBC system [9].

The oxidation resistance and the TGO quality depend not only on the chemical composition but also on the method used to produce the bond coats. MCrAlY coatings can be realized by several thermal spraying techniques (VPS, APS, LPPS, HVOF). VPS (Vacuum Plasma Spraying) represents the state of the art technology for the industrial bond coat deposition, but the costs are relatively high due to the vacuum operation conditions. VPS avoids the powder oxidation during the spraying and the consequent consumption of the aluminium reservoir of the coating before service life.

HVOF spray systems work at atmospheric pressure therefore the investment and operation costs are much lower [10-13]. Recent researches has showed the potential of HVOF compared to VPS [14]. Other studies attribute to the HVOF process the capability of forming a fine Al_2O_3 dispersion during the spraying process [15]. Alumina nuclei present in the as-deposited coating seems to have a beneficial effect on the oxidation resistance by promoting the growth of a protective TGO layer or slowing down aluminium diffusion into the substrate acting as a diffusion barrier. The HVOF spraying of powders with high oxygen affinity could result in the industrial production of bond coats with higher oxidation resistance properties and lower costs.

In the present work, two different bond coats of comparable thickness, were deposited onto a superalloy substrate by means of an HVOF system, using two different CoNiCrAlY powders with approximately the same chemical composition and granulometry, but showing different reactivity toward oxygen. After deposition, samples were isothermally oxidized at 1,273 K for different periods of time up to 5,000 hours. Before and after the furnace tests, samples were extensively characterized. The different properties and characteristics of the powders and the coatings were analyzed and discussed.

The aim of the present work was to investigate how the initial powder reactivity toward oxygen can affect the final oxidation behaviour of bond coats produced by HVOF technique and corroborate the results shown in our previous paper [16].

2. Results and Discussion

2.1. Powder Characterization

The compositions of the powders were very similar, except for the presence of small quantity of silicon and calcium in the powder B.

The powder granulometry ranged between 15–45 μm for both the powder types. The powders show a spherical morphology (Figure 1) and mainly consisted of two metallic phases ((γ-(Co,Ni) and β-(Co,Ni)Al)) as shown in Figure 2.

Figure 1. SEM micrographs of the powders A and B.

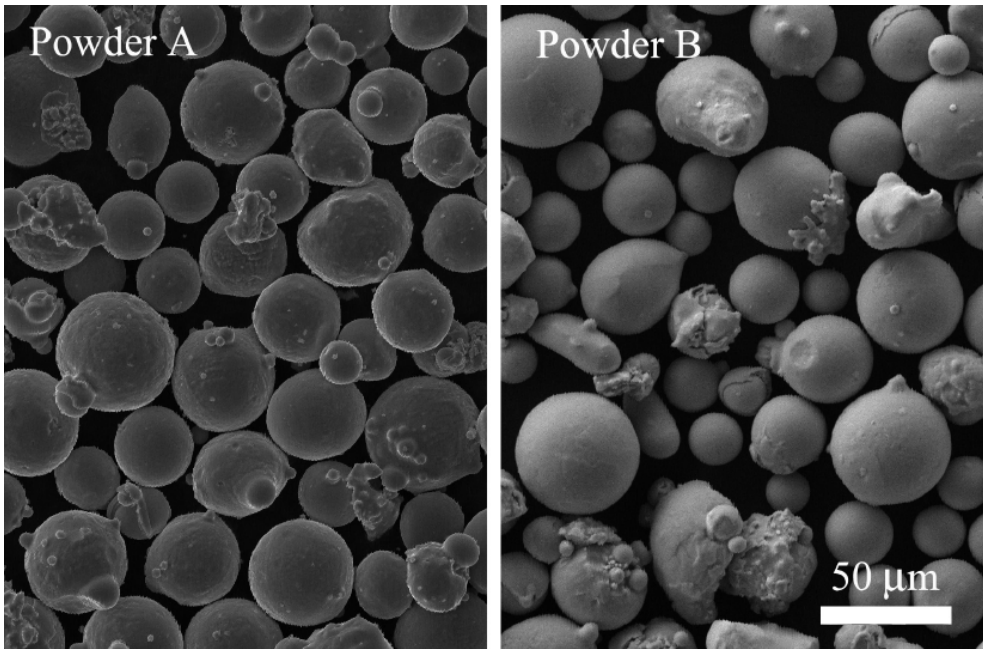

Figure 2. XRD patterns for powders A and B.

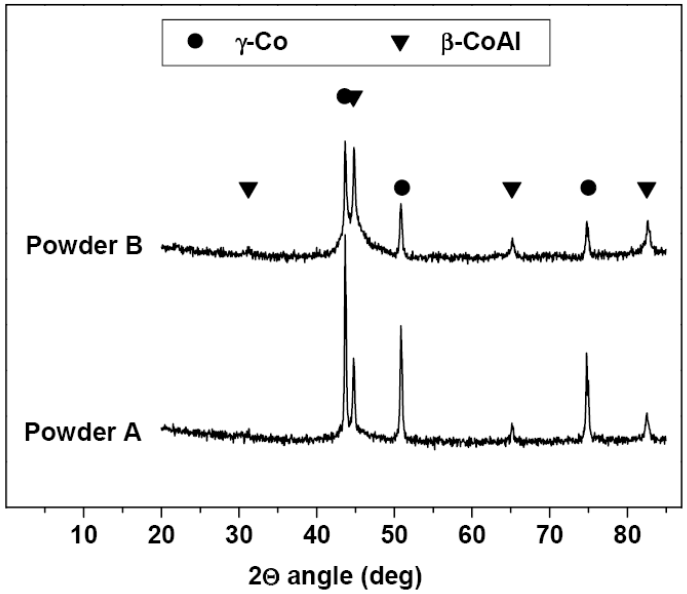

It should to be noted that, even if the particle size of the two powders is comparable, the crystallite size of powder B was smaller in comparison with powder A, as revealed by the broadening of the diffraction peaks (Figure 2). In Figure 3 the TGA analysis results are shown.

Figure 3. Comparison between TGA curves (at 1,273 K) of powders A and B.

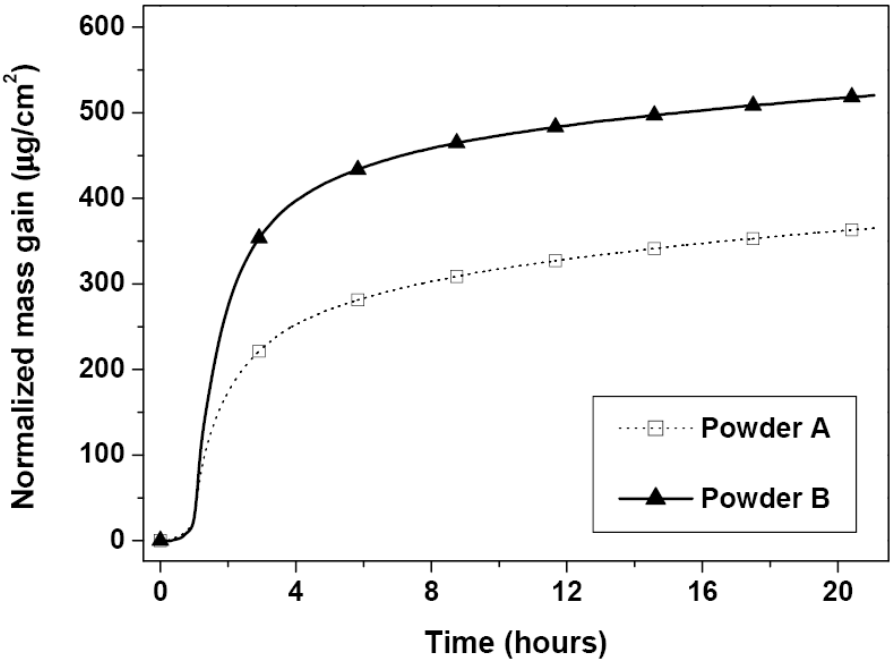

The graph shows a higher mass gain in the case of powder B. Particularly, the mass gain is concentrated during the first stages. This behaviour would suggest that, during the spraying, powder B tends to oxidize much more readily in respect to powder A [16]. Generally, this feature is not considered beneficial for the durability of coatings, as it is thought that aluminium oxidises during the spraying resulting in depletion of the aluminium reservoir even before the components enters service life. This consideration in the past has promoted the use of VPS in order to reduce the powder oxidation during the spraying. Following the results obtained in previous works [14,16] we hypothesized that by using HVOF a powder with a starting higher reactivity toward oxygen could improve the initial quality of the TGO and thus promote a higher oxidation resistance.

2.2. Bond Coat Characterization

Bond coats obtained by spraying powder A and B will be hereafter respectively named samples A and samples B. Results will be comparatively presented for each type of the studied features.

2.2.1. Al depletion zones and TGO growth

In Figure 4 some micrographs of the sample cross sections, obtained before and after different oxidation periods of time, are reported.

Figure 4. Optical micrographs of the cross sections of the samples produced with powder A and B after different periods of oxidation at 1,273 K.

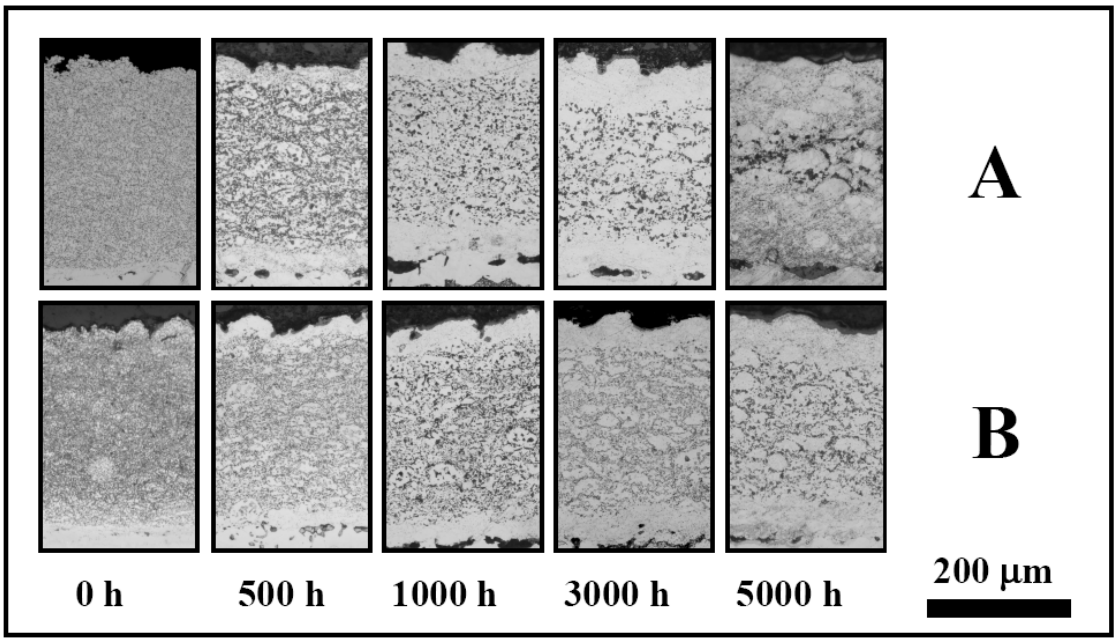

The overall thickness of the sample bond coats was about 300 μm. The as-coated samples showed that both the γ and β phases present in the powders. A thin interdiffusion layer (about 20 μm) was detected between the bond coat and the superalloy substrate. During oxidation, aluminium diffused out of the CoNiCrAlY coating surface to form the TGO layer and into the substrate, promoting outer and inner β-(Co,Ni)Al depletion. The aluminium depletion zone thickness increased during the tests.

Figure 5 shows the thickness of the outer and inner aluminium depleted zones before and during the oxidation tests.

EDX analysis performed in the central aluminium rich zones of both the samples showed an aluminium concentration comparable to initial values. In the case of samples of type A, after 5,000 h at 1,273 K, the aluminium reservoir is reduced to about one third of the initial. The residual life of the bond coats produced by powder A, before the start of severe oxidation with Cr_2O_3 formation, could be reasonably estimated to be about an additional 3,000 h. On the contrary, in the case of samples B, the aluminium reservoir is hardly consumed; after 5,000 h of oxidation test the aluminium depleted zone thickness of sample B are comparable to those of samples A after only about 2,000 h of testing. For this, the residual life of the bond coats produced by powder B could be reasonably estimated to be about an additional 10,000 h.

Both inner and outer aluminium depleted zones of samples B, showed a slower increasing rate in comparison with sample A. The slower growth rate of the outer zone could be correlated to a higher oxidation resistance of sample B, due to a more protective TGO, which allows a smaller aluminium consumption from the reservoir.

Figure 5. Thickness of the inner and outer aluminium depletion layers of samples A and B before and after different periods of oxidation at 1,273 K.

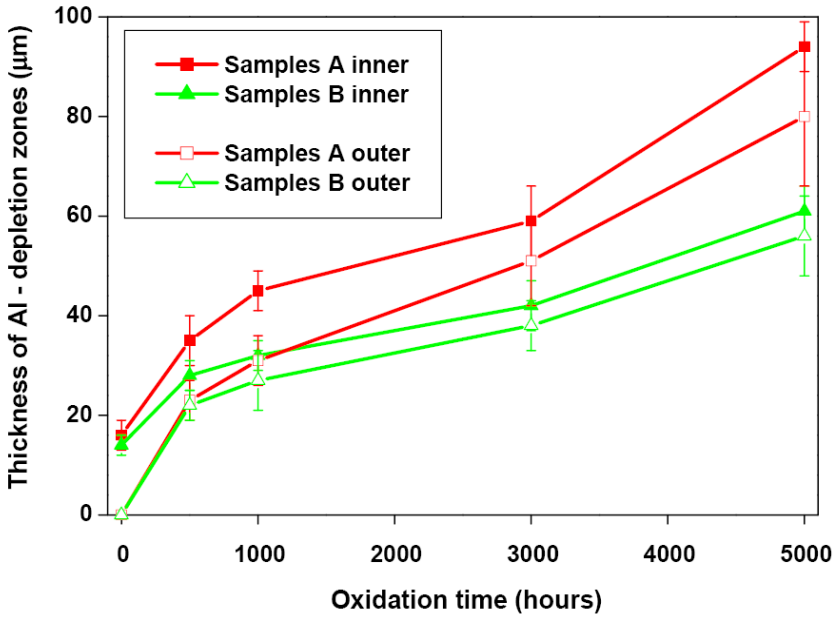

The reduced diffusion into the bulk cannot be simply explained in terms of oxidation resistance, because diffusion depends only on the concentration gradient and on the aluminium diffusion coefficients. In our case the compositions of the coatings are comparable, thus the gradient concentration can be reasonably considered approximately the same in both types of samples. In this sense, the fact that aluminium diffuses into the bulk at a lower rate in the case of samples B could be reasonably ascribed only to lower apparent diffusion coefficients. Lower apparent diffusion coefficients could be related to the formation of a diffusion barrier layer between the splats during the spraying. Probably, powder B, which is easily oxidized during the spray process, is able to produce, during time of flight, a thin aluminium oxide layer which works as a diffusion barrier and decreases the aluminium flux through the coating toward the substrate.

Moreover, each sample showed inner depletion layers not much thicker than the outer ones. This behaviour can be ascribed to the small Al concentration gradient between the bond coats and substrate. By using a superalloy substrate containing less aluminium percentage the service life of the coatings could be reduced by increasing the rate of aluminium diffusion into the bulk and producing inner depletion layers thicker than the outer ones, as observed in our previous work [16].

In Figure 6 the thickness evolution of the TGO layer of the two different coating types are reported. It has to be highlighted that the measurements were performed where no evident fracture and oxide spalling from the bond coat were detected. The TGO thickness of both samples was about the same, considering the dispersion value, nevertheless in the case of samples A it has to be noted that the TGO layer were always a little thinner. Both the sample types showed a bi-layer structured TGO.

Figure 6. Thickness of TGO layers of samples A and B after different periods of oxidation at 1,273 K.

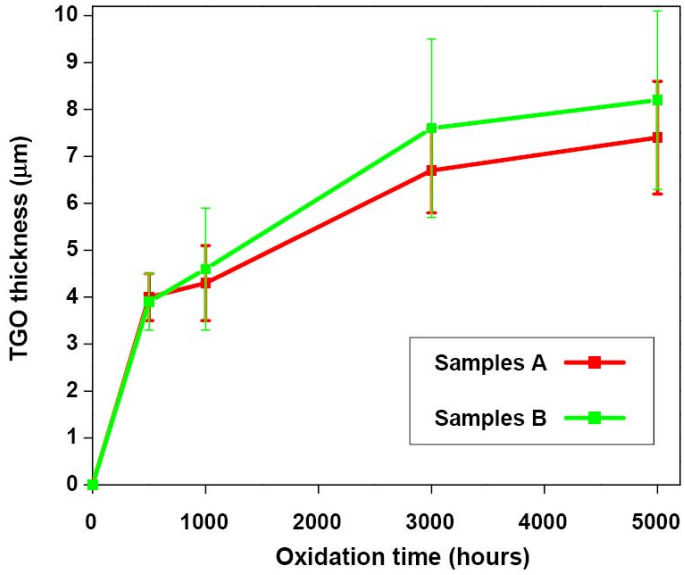

EDX spectra reported into Figure 7 showed that the inner TGO layers were mainly formed by aluminium oxide, while the outer TGO layer contained other metallic oxides (Cr and Ni rich oxide). SEM observations performed with back-scattered electrons signal showed that the aluminium oxide TGO inner layers showed about the same thickness for both the sample types, while the thickness of the TGO outer mixed oxide layers were different. Particularly, the thickness of the outer mixed oxide TGO layers were thinner in the case of samples A; the last feature was the main reason of the lower total TGO thickness of samples A. It can be hypothesized that the lower thickness of outer TGO layer could be correlated to a lower cohesion and compactness of these layers in comparison with those formed on the surface of the samples B; presumably the outer TGO layers of samples A are more subject to delamination and their measured thickness appear lower.

2.2.2. Surface Modifications

Figure 8 shows a picture which allows visual comparison of the surfaces of the samples before and after the oxidation test. Before the test, the bond coats had a metallic appearance. Oxidation generates a blue coloration, due to the presence of cobalt which reacts with oxygen.

Visual inspection of sample A revealed TGO delamination after 3,000 h of testing, when a large percentage of surface oxide spalled and the surface lost the prevalent blue coloration. In comparison, sample B, did not show appreciable delamination signs or relevant oxide spallation even after 5,000 h of testing. It is reasonable to think that most of the delamination occurred during cooling down to room temperature, despite the very low cooling rate. Thus, visual inspection allows to coarsely evaluate the higher adhesion of the TGO layers formed onto samples B in comparison with samples A.

Figure 9 shows SEM micrographs of the surface of the coated samples before and after different oxidation periods. The coatings showed a rough surface, due to the overlap of different splats and to the roughness of each single splat. As the oxidation time increases, nucleation and growth of the oxide

scale becomes more and more relevant, as shown by the sample charging under the electron beam. Moreover, some delamination of the TGO layers can be observed. Accordingly to the visual inspection samples A show larger detached areas in comparison with samples B.

Figure 7. The TGO bi-layered structure relative to sample B oxidized at 1,273 K for 5,000 h. The arrows indicate the regions where EDX analyses were performed.

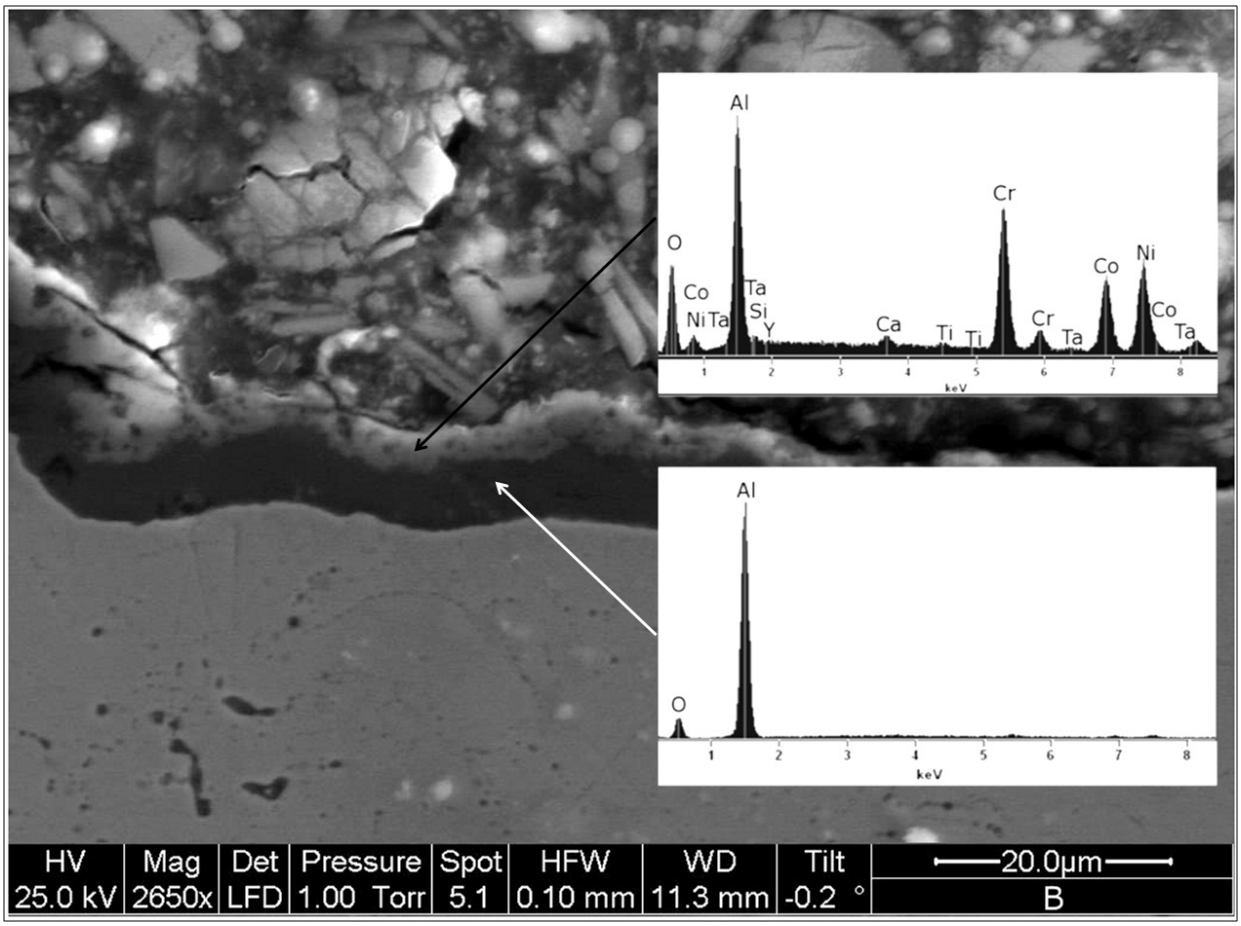

Figure 8. Picture showing the typical appearance of samples A and B before and after different periods of oxidation at 1,273 K.

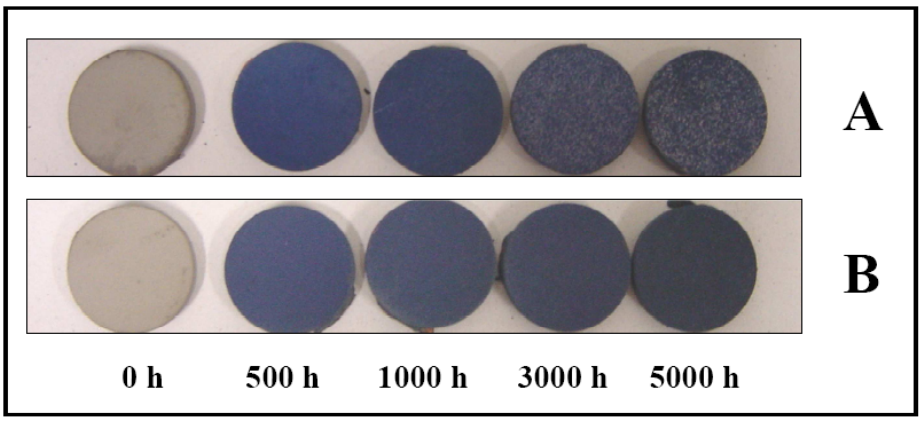

Figure 9. SEM micrographs showing the morphology evolution of the surface of samples A and B before and after different periods of oxidation at 1,273 K.

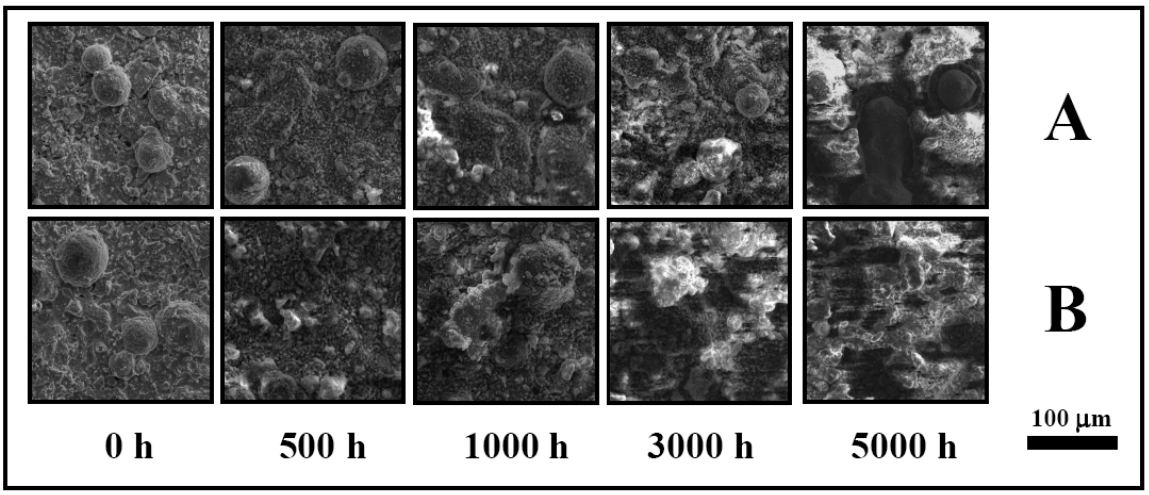

Figure 10. (a) XRD patterns of the surface of samples A before and after different periods of oxidation at 1,273 K. **(b)** XRD patterns of the surface of samples B before and after different periods of oxidation at 1,273 K.

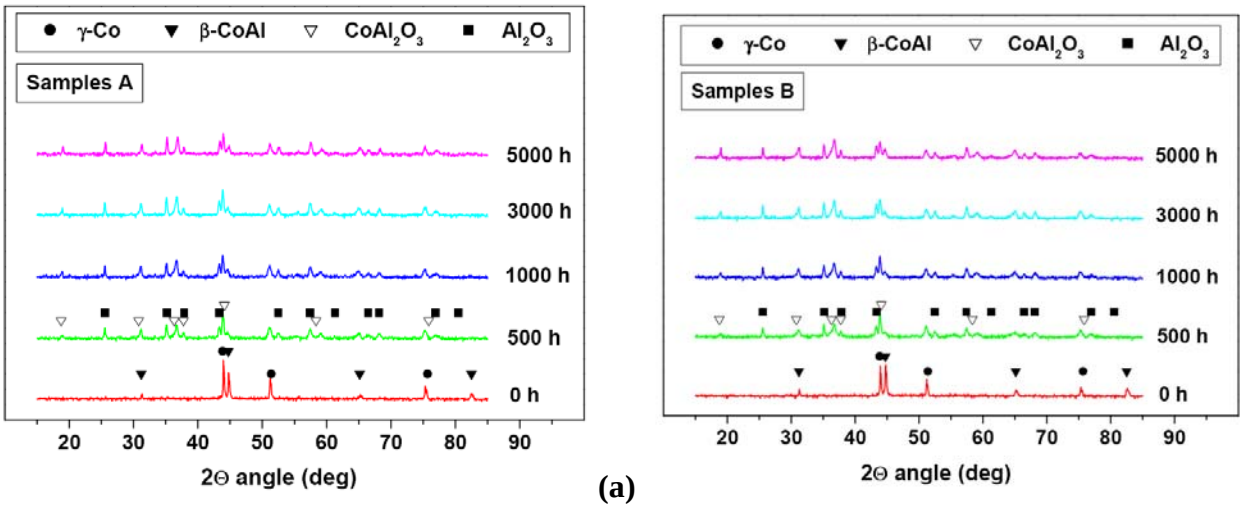

Figures 10a and 10b show the XRD patterns of tested and untested bond coats. The analysis performed on the unoxidized samples showed the presence of both γ-(Co,Ni) and β-(Co,Ni)Al. Oxidized sample XRD patterns, indicated that the oxide scale mainly constituted of α-Al_2O_3 and $(Co,Ni)(Cr,Al)_2O_4$ spinel for each sample type even after 5,000 hours of oxidation testing. No Cr_2O_3 peaks were detected, according to the cross sectional analysis which did not show any evidence of severe oxidation phenomena.

Figure 11 shows EDX analysis results relative to the surface of tested and untested samples. Untested samples showed surface aluminium concentration higher than that of the nominal powder composition due to the preferential aluminium oxidation during the spraying or the low vacuum interdiffusion treatments. These oxide layers are certainly very thin (presumably less than 0.3 µm),

in agreement with XRD analysis and the visual inspection did not detect a significant amount of oxides. During the first 500 h of the oxidation tests the aluminium surface concentration increases due to oxide scale formation. After this initial period, the compositional analysis showed that the aluminium and nickel content decreased and increased respectively, while Co and Cr showed less relevant variations. After 5,000 h, the aluminium and nickel or chromium concentrations of samples A respectively are higher and lower in comparison with those of samples B. The higher concentration values of chromium and nickel and the lower aluminium concentration values detected on the surface of samples B are in agreement with the morphological observations and the diffraction analyses relative to the TGO layers; samples B showed thicker outer mixed oxide TGO layers and this is the reason why the X-ray signals collected from the inner alumina layers are less significant in comparison with those of samples A.

Figure 11. (a) Surface composition measured by EDX analysis of samples A before and after different periods of oxidation at 1,273 K. **(b)** Surface composition of samples B before and after different periods of oxidation at 1,273 K.

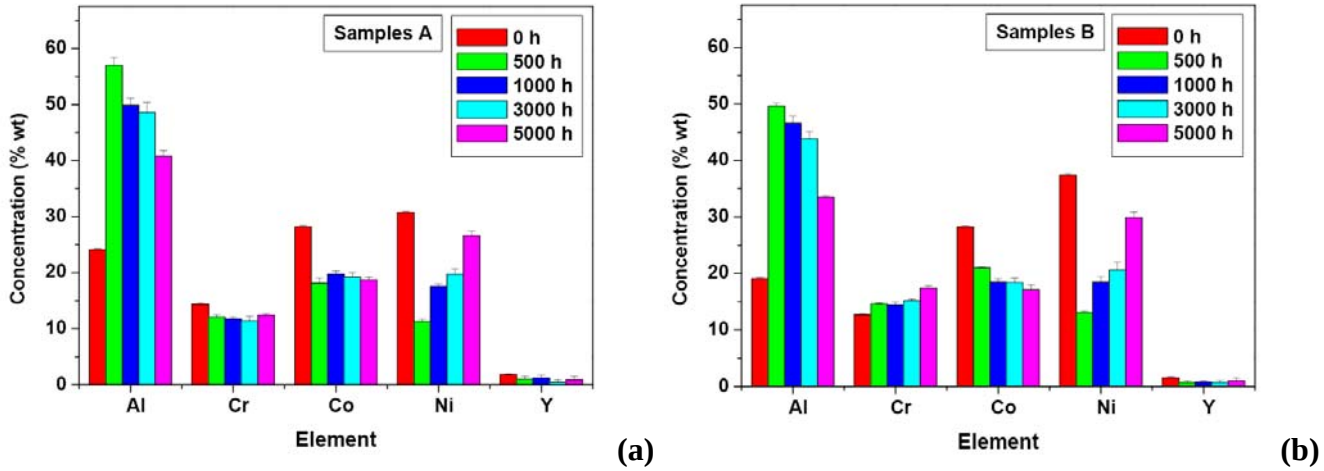

2.2.3. Electrochemical Impedance Spectroscopy measurements

In this work the main interest is the simple comparison of the different EIS curves, measured after different oxidation periods, onto the 2 different coating types. The aim was to obtain some general considerations about the growth and the quality of the TGO layers. For this reason, EIS results will be not presented trying to fit data with some electrical equivalent circuit.

Figure 12 shows that the electrochemical impedance values of samples A increased passing from the untreated samples to the samples oxidized for 1,000 h; after this time the impedance values decreased. Particularly, samples oxidized for 3,000 h showed impedance values only a little higher than the untreated samples and samples oxidized for 5,000 h showed impedance values comparable with those of the untreated ones.

Figure 12. EIS Bode plot of samples A and B before and after different periods of oxidation at 1,273 K.

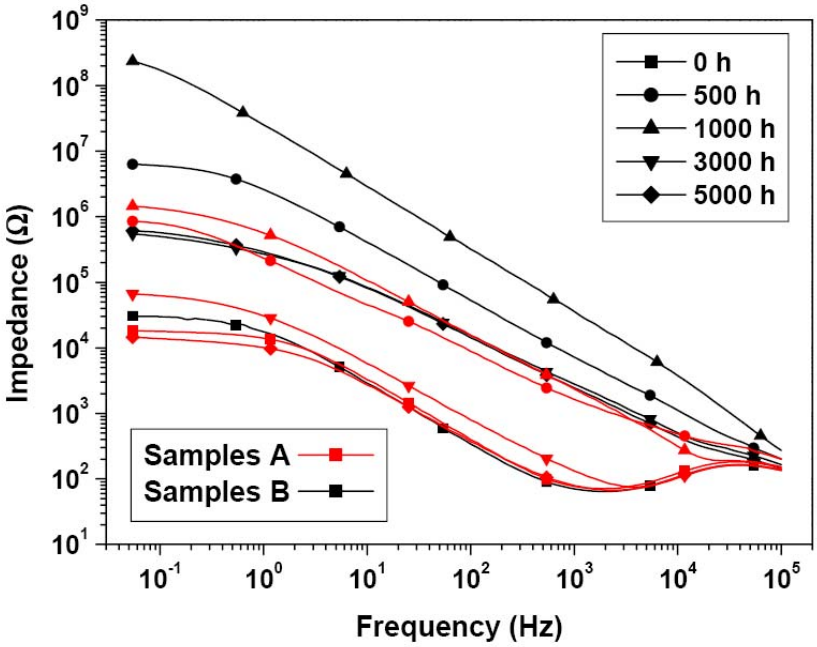

In the case of samples B a different behaviour was observed. The electrochemical impedance values increased passing from the untested samples to the samples oxidized for 500 h and reaches the maximum values at 1,000 h. Then the impedance values decreased, but even in the case of samples oxidized for 5,000 h the impedance values are higher than those of the untreated samples. Moreover, it has to be noted that the maximum impedance values of samples B, at a fixed frequency, are about 2 orders of magnitude higher in comparison with those of samples A. The impedance values of a dielectric material coating can be primarily correlated with its thickness and quality. TGO should be an insulating layer. A compact and almost defect free TGO layer increases the electrochemical impedance values of the samples as its thickness increases, due to the lowering of the electrical capacity and to the increasing of its electrical resistance. It can be hypothesized that the impedance values of samples with a delaminated or a low quality TGO layer are between those samples with a defect free TGO layer and the bare substrate without any oxide layer. In this sense the different electrochemical behaviour of samples A and B could be mainly ascribed to the differences of quality and adhesion of the two different coatings.

Samples B showed a higher quality TGO layer; their thickness increase produced a higher impedance value. After 1,000 h of testing the measured TGO thicknesses were comparable, but the impedance value absolutely did not.

In the case of samples A, even if there is a TGO thickness increment, this is presumably accompanied by delamination, cracks and porosity formation just after the first periods of the test. It is reasonable to hypothesize that samples A showed a large decrease in impedance values after 1,000 hours of testing due to the loss of adhesion and quality. This effect led to electrochemical values averaged between a defect-free TGO impedance values and those of the damaged zones. According to

visual and microscopic inspections, samples A after 3,000 h of testing showed a surface with a very large percentage of delamination , while samples B did not up to 5,000 h. The large TGO delamination can explain impedance values very similar to those of the unoxidized samples.

Finally, it has to be highlighted that electrochemical impedance analysis is a valuable tool in order to assess the quality of the TGO layer. Particularly its sensitivity is higher in comparison with visual inspection, microscopic techniques or XRD analysis. These results support the idea that EIS analysis can be used as a non destructive evaluation instrument in order to study the residual life of complete TBC systems.

3. Material and Methods

Inconel 738 nickel based superalloy (nominal composition: Ni balance, Cr-15.9, Co-8.5, Al-3.5, Ti-3.5, W-2.5, Mo-1.9, Ta-1.7 (%wt)) disk samples (ϕ 25 mm), were used as substrates. Before deposition, the substrates were grit blasted using corundum with a grain size of 60–80 mesh, in order to remove surface oxides and to obtain a suitable roughness for coating adhesion.

The composition of the two CoNiCrAlY powders (hereafter named "A" and "B") are reported in Table 1.

Table 1. Chemical composition of the powders A and B.

Powder type	**%Co**	**%Ni**	**%Cr**	**%Al**	**%Y**	**%Ca**	**%Si**
A	balance	31.3	20.9	8.0	0.5	-	-
B	balance	32.0	21.1	8.3	0.5	0.09	0.03

The as-received powders were characterized by X-ray diffraction (XRD), scanning electron microscopy (SEM), energy dispersive X-ray microanalysis (EDX) and thermal gravimetric analysis (TGA). TGA was performed at 1,273 K in air (flux: 20 ml/min, heating rate to the temperature set point: 15 K/min) for about 20 hours recording the mass gain due to the oxide layer formation. Weight gains for each kind of powder were normalized considering the total surface area exposed to the aggressive environment. The total area was estimated by the data obtained by means of laser granulometric analysis.

The torch used to manufacture the bond coats was a liquid fuelled gun (Tafa/Praxair JP5000); the powder injection was radial and the gas flow was obtained by the combustion between oxygen and kerosene.

After spraying, all the samples were vacuum interdiffused for 2 hours at 1,423 K.

Isothermal oxidation tests of the two different coated specimen types were conducted at the same time and in the same high temperature furnace at 1273 K in air, in order to assure identical test conditions. Samples were analyzed before and after 500, 1,000, 3,000 and 5,000 hours of testing. The cooling down of the samples was carried out inside the furnace reaching room temperature after about 1 day; the furnace temperature was decreased step by step (steps of 50 K) from 1,273 K to 773 K changing the set-point of the furnace PID control (it took some hour). Below 773 K the furnace was turned off and the sample cooled freely into the furnace itself.

The average thickness of the coatings, the interdiffusion layer and Al depletion layers were measured by optical and scanning electron microscopy (SEM). The surface morphology and the chemical composition of the as-coated and oxidized samples were examined by SEM-EDX. In order to determine the crystalline structure and estimate the relative amount of the main surface phases XRD analysis (Bragg-Brentano configuration using Cu-Ka radiation) were performed on the surface of the coatings before and after the different oxidation exposure times.

EIS (electrochemical impedance spectroscopy) analysis was performed before and after 500, 1,000, 3,000 and 5,000 hours of test. The measurements were carried out at room temperature in a conventional three-electrode system in a flat cell with a volume of 300 ml on 3 different samples for each sample type in order to assess the reproducibility. Coated samples were used as working electrodes exposing to the electrolyte an area of 1 cm^2. A platinum mesh was used as a counter electrode and a KCl-saturated Calomel electrode was used as reference. $K_3Fe(CN)_6/K_4Fe(CN)_6$ aqueous solution (0.01 M) was employed as electrolyte, because of its highly reversible electrochemical exchange current density and minimal interference with the system [17]. A sinusoidal voltage perturbation of 15 mV amplitude and a frequency range of 50 mHz–100 kHz was selected. EIS measurements were recorded at the open circuit potential after a delay period from 1 to 24 hours in order to assess the stability of the system.

4. Conclusions

In this work isothermal high temperature oxidation tests of CoNiCrAlY bond coats of comparable thickness produced by HVOF onto Inconel 738 substrates were carried out. The two powders used to produce the different coatings had approximately the same chemical composition and granulometry, but different reactivity towards oxygen.

Before and after the oxidation tests, morphological, microstructural, compositional and electrochemical analyses were performed in order to produce a complete characterization. The two powders showed considerable differences in their behaviour. Bond coats deposited using powders with higher starting reactivity toward oxygen resulted in higher oxidation resistance in comparison to the others . This behaviour could be ascribed to the formation of alumina precursor nuclei on the splat surface which promotes adherent and very good quality oxide scale growth acting, in a very effective way, as a diffusion barrier of aluminium toward the substrate.

Acknowledgements

This work was supported by the FIRB Project n°RBIP06X7F4.

References and Notes

1. Evans, A.G.; Mumm, D.R.; Hutchinson, J.W.; Meier, G.H.; Pettit, F.S. Mechanisms controlling the durability of thermal barrier coatings. *Prog. Mater. Sci.* **2001**, *46*, 505-553.
2. Shillington, E.A.G.; Clarke, D.R. Spalling failure of a thermal barrier coating associated with aluminum depletion in the bond-coat. *Acta Mater.* **1999**, *47*, 1297-1305.

3. Brandl, W.; Grabke, H.J.; Toma, D.; Krüger, J. The oxidation behaviour of sprayed MCrAlY coatings. *Surf. Coat. Technol.* **1996**, *86-87*, 41-47.
4. Padture, N.; Gell, M.; Jordan, E. Thermal barrier coatings for gas-turbine engine applications. *Science* **2002**, *296*, 280-284.
5. Stiger, M.J.; Yanar, N.M.; Toppings, M.G.; Pettit, F.S.; Meier, G.H. Thermal barrier coatings for the 21st century. *Z. Metall.* **1999**, *90*, 1069-1078.
6. Clarke, D.R.; Levi, C.G. Materials design for the next generation thermal barrier coatings. *Annu. Rev. Mater. Sci.* **2003**, *33*, 383-417.
7. Miller, R.A. Thermal barrier coatings for aircraft engines: History and directions. *J. Therm. Spray Technol.* **1997**, *6*, 35-42.
8. Busso, E.P.; Lin, J.; Sakurai S.; Nakayama, M. A mechanistic study of oxidation-induced degradation in a plasma-sprayed thermal barrier coating system: Part I: Model formulation. *Acta Mater*. **2001**, *49*, 1515-1528.
9. Chen, W.R.; Wu, X.; Marple, B.R.; Nagy, D.R.; Patnaik, P.C. TGO growth behaviour in TBCs with APS and HVOF bond coats. *Surf. Coat. Technol.* **2008**, *202*, 2677-2683.
10. Brandl, W.; Toma, D.; Kruger, J.; Grabke H.J.; Matthaus, G. The oxidation behaviour of HVOF thermal-sprayed MCrAlY coatings. *Surf. Coat. Technol.* **1997**, *94-95*, 21-26.
11. Toma, D.; Brandl, W.; Köster, U. Studies on the transient stage of oxidation of VPS and HVOF sprayed MCrAlY coatings. *Surf. Coat. Technol.* **1999**, *120-121*, 8-15.
12. Taylor, R.; Brandon, J.R.; Taylor, R.; Morrell, P. Microstructure, composition and property relationships of plasma-sprayed thermal barrier coatings. *Surf. Coat. Technol.* **1992**, *50*, 141-149.
13. Lugscheider, E.; Herbst, C.; Zhao, L. Parameter studies on high-velocity oxy-fuel spraying of MCrAlY coatings. *Surf. Coat. Technol.* **1998**, *108-109*, 16-23.
14. Di Ferdinando, M.; Fossati, A.; Lavacchi, A.; Bardi, U.; Borgioli, F.; Borri, C.; Giolli, C.; Scrivani, A. Isothermal oxidation resistance comparison between air plasma sprayed, vacuum plasma sprayed and high velocity oxygen fuel sprayed CoNiCrAlY bond coats. *Surf. Coat. Technol.* **2010**, *204*, 2499-2503.
15. Yuan, F.H.; Chen, Z.X.; Huang, Z.W.; Wang, Z.G.; Zhu, S.J. Oxidation behavior of thermal barrier coatings with HVOF and detonation-sprayed NiCrAlY bondcoats. *Corros. Sci.* **2008**, *50*, 1608-1617.
16. Fossati, A.; Di Ferdinando, M.; Lavacchi, A.; Bardi, U.; Giolli, C.; Scrivani, A. Improvement of the isothermal oxidation resistance of CoNiCrAlY coating sprayed by High Velocity Oxygen Fuel. *Surf. Coat. Technol.* **2010**, *204*, 3723-3728.
17. Gómez-García, J.; Rico, A.; Garrido-Maneiro, M.A.; Múnez, C.J.; Poza, P.; Utrilla, V. Correlation of mechanical properties and electrochemical impedance spectroscopy analysis of thermal barrier coatings. *Surf. Coat. Technol.* **2009**, *204*, 812-815.